

# Patient-Specific Study of a Stenosed Carotid Artery Bifurcation Using Fluid–Structure Interactive Simulation

Nelson Pinho<sup>1</sup>, Marco Bento<sup>1</sup>, Luísa C. Sousa<sup>2(✉)</sup>, Sónia Pinto<sup>3</sup>, Catarina F. Castro<sup>2</sup>, Carlos C. António<sup>2</sup>, and Elsa Azevedo<sup>4</sup>

<sup>1</sup> DEMec, FEUP, Universidade do Porto, Porto, Portugal

<sup>2</sup> INEGI-DEMec, FEUP, Universidade do Porto, Porto, Portugal  
lcsousa@fe.up.pt

<sup>3</sup> Faculdade de Engenharia da, Centro de Estudos de Fenómenos de Transporte (CEFT),  
Universidade do Porto, Porto, Portugal

<sup>4</sup> H. São João-FMUP, Universidade do Porto, Porto, Portugal

**Abstract.** Atherosclerosis at the carotid bifurcation is a major risk factor for stroke. A computational model incorporating transient wall deformation of carotid arteries was developed to assess the influence of artery compliance on wall shear stress (WSS). Clinical data was obtained from ultrasound technique. Two patients were studied, one presenting a mild-graded carotid stenosis along internal carotid artery (ICA) and the other with no visible stenosis. It is hoped that patient-specific biomechanical analyses will help diagnosis and to assess the rupture potential for any particular lesion.

**Keywords:** Patient-specific · Image-based · Atherosclerosis · Risk assessment · Fluid-structure interaction

## 1 Introduction

Atherosclerotic plaques and wall thickenings are localized in major bifurcations as the common carotid artery (CCA) bifurcation. The focal distribution of atherosclerosis is believed to be linked to hemodynamic factors. Several studies have attempted to correlate low and oscillating WSS regions with regions of increased intimal thickness and atherosclerotic plaque development in CCA bifurcation [1–3]. Stenosis can lead to critical flow alterations such as high flow velocities, high shear stress and flow recirculation, which may be linked to thrombus formation and stroke [3]. The rupture of carotid atherosclerotic plaques is a major cause of cerebrovascular thrombotic events, and this mechanism is not fully understood.

2D and 3D patient-specific finite element models of diseased vessels have been used to investigate the mechanics of atherosclerotic vessels and to assess the rupture vulnerability for carotid bifurcation lesions [4–9]. Recent studies [10, 11] suggest that a local increase in stress/strain could be a cause of plaque rupture, and that stress in the plaque region can be used for plaque rupture risk assessment. Fluid-Structure Interaction (FSI) allows blood flow simulations, where both fluid and structural solution domains are

coupled using computational fluid dynamics (CFD) and Finite element methods respectively. Results from both the analysis are exchanged at interface junction. In this work FSI analysis is employed in order to determine flow and wall stress distributions and to investigate the effect of stresses on carotid atherosclerotic plaque. As the carotid system is quite superficial it can be examined with a high-frequency transducer yielding B-mode images with high spatial resolution, useful to identify the lumen of the arteries and their walls. Ultrasound images were also used to define patient-specific flow boundary conditions at the CCA inlet.

Such simulations are complex, and suffer from major challenges: models are based on medical imaging and material responses for plaque and vessel tissues are difficult to obtain on a patient-specific basis; the boundary conditions are often rough approximations of the *in vivo* situation. Additionally, the generation of a suitable computational mesh that can accurately represent the components of the diseased artery and provide meaningful numerical solutions, demands high computational resources to solve realistic finite/volume element models based on a patient-specific geometry, rendering it not acceptable for clinical practice.

In this paper, a patient specific 3D FSI simulation is carried out using ANSYS® commercial software throughout its coupling system feature. The main goal of this study is to investigate the hemodynamic characteristics on the distribution of wall shear stress and WSS descriptors, induced by the arterial wall deformation. Rigid and FSI models of a healthy and a stenosed common carotid artery bifurcation are presented and compared. Due the cardiac pressure, the blood flow distends the elastic artery and deformed artery affects the flow behaviour. The elastic nature of the arterial wall determines the magnitude of the elastic recovery and FSI simulations show different behaviour for each common carotid bifurcation studied.

## 2 Materials and Methods

Clinical data is obtained from ultrasound technique studies at the Neurosonology Unit of the Department of Neurology of Hospital São João in Portugal. A protocol for this study has been approved by the local institutional ethical committee and informed consent of each volunteer was obtained. The geometry definition of the carotid artery bifurcation was based on Ultrasound patient-specific data. A set of Doppler images of the CCA, its bifurcation and proximal segments of ICA and external carotid artery (ECA) were acquired during daily medical routine. B-mode images were segmented to produce smooth lumen and atherosclerotic plaque contours by using a segmentation method based on the hypoeogenic characteristic of the lumen; the in-house semi-automatic algorithm implemented in MATLAB software allows the lumen and plaque contour extraction in 2D longitudinal and transversal B-mode images [12]. The reconstruction of the arterial regions was performed placing 2D smooth lumen contours in the axial direction according to each image location obtained during data acquisition (Fig. 1). After smoothing of the obtained surface, three diameters cylindrical extensions upstream and downstream of the carotid bifurcation were performed, such that flow could be modeled with reasonable boundary conditions.

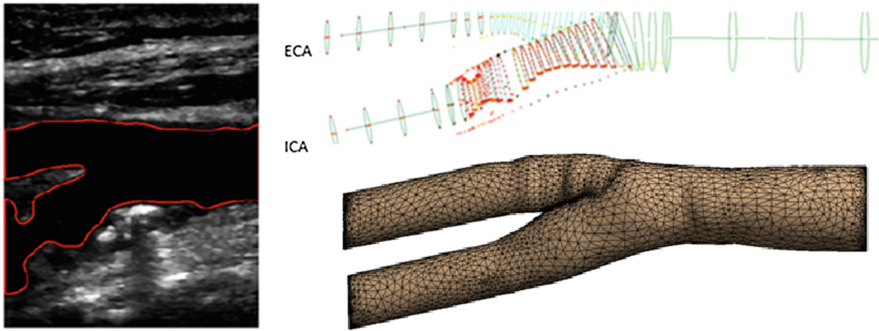


**Fig. 1.** Segmented longitudinal image and wall surface reconstruction

A Tetrahedral mesh (finite volumes) was generated using the software Ansys Fluent. A temporal and spatial mesh refinement were performed, considering a mesh sensitivity analysis based on maximum nodal WSS (variations lower than 5%). The obtained mesh with 93989 nodes and 492083 elements was sufficient to resolve the fluid pressure field to a good approximation. Blood flow simulation was obtained iteratively, using the SIMPLE algorithm and a second-order upwind scheme for the convective terms. Blood was considered an incompressible homogeneous non-Newtonian fluid, with the rheological behavior described by Carreau model and a density of  $1060 \text{ kg/m}^3$ . A propose-developed MatLab code was used to calculate the time-dependent Womersley velocity profile based on Doppler ultrasound measurements at the CCA inlet section [2]. For the ICA and ECA outlets a time-varying pressure, simulating blood pressure during cardiac cycle, is used as flow boundary condition (Fig. 2).

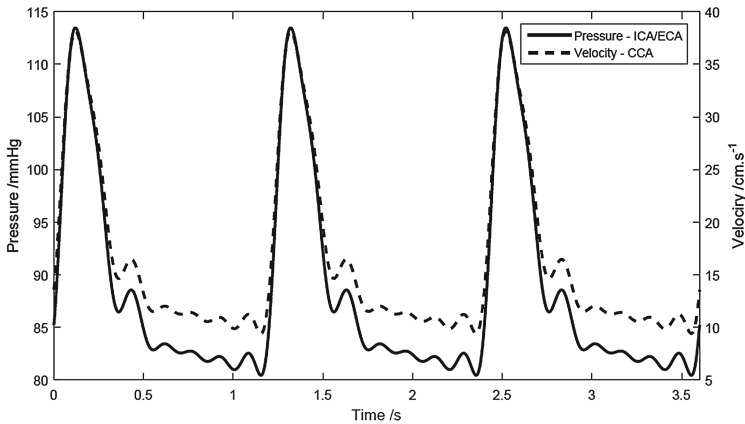


**Fig. 2.** Flow velocity and pressure waveforms.

The arterial wall was modeled as an isotropic elastic material with a Young's modulus of 1.2 MPa, a Poisson's ratio  $\nu = 0.4$  and a density equal to  $1120 \text{ kg/m}^3$ . The thickness of the blood vessel wall was considered equal to 1.5 mm [7]. The

atherosclerotic plaque was modeled as an isotropic material with a Young's modulus of 9.5 MPa, a Poisson's ratio  $\nu = 0.27$  and a density equal to 1220 kg/m<sup>3</sup> [11, 13]. A Tetrahedral mesh (finite elements) was generated using the transient mechanical software available in Ansys Workbench. Final mesh was composed by 188327 nodes and 122024 elements for the discretization of the arterial walls and 178308 nodes and 108743 elements for the plaque. All degrees of freedom from of all nodes on the inlet and outlet planes were constrained. Remaining nodes were left free to undergo displacement in any direction [6] (Fig. 3).

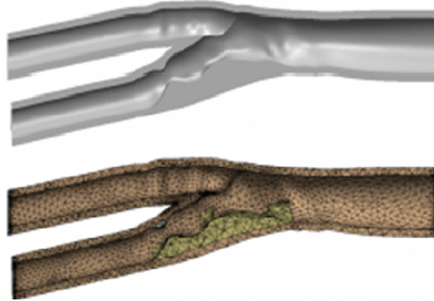
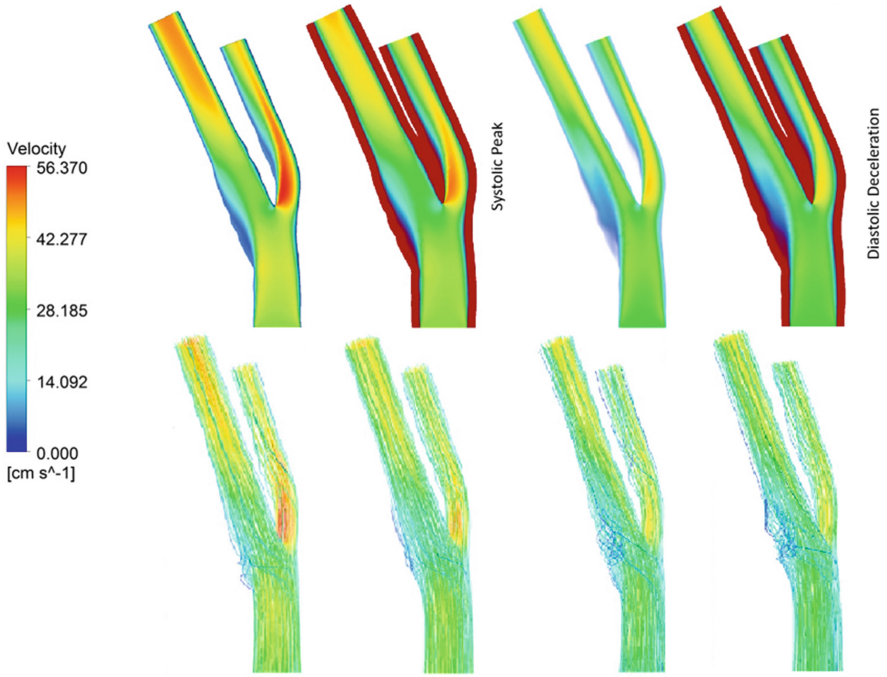


**Fig. 3.** Arterial wall and plaque mesh.

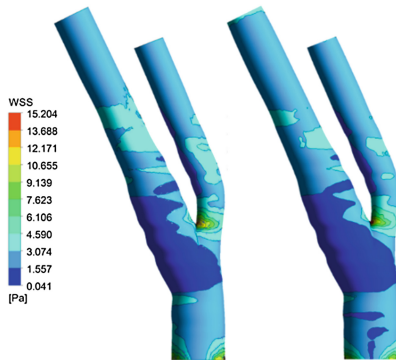
FSI simulation was performed in a computer running Intel® Core i7-7700 K @ 4.2 Ghz and 32 Gb of RAM. Three cardiac cycles were simulated considering a constant time step equal to 0.008 s. The flow velocities and the WSS vectors obtained from the last cycle were recorded for post-processing.

### 3 Results and Discussion

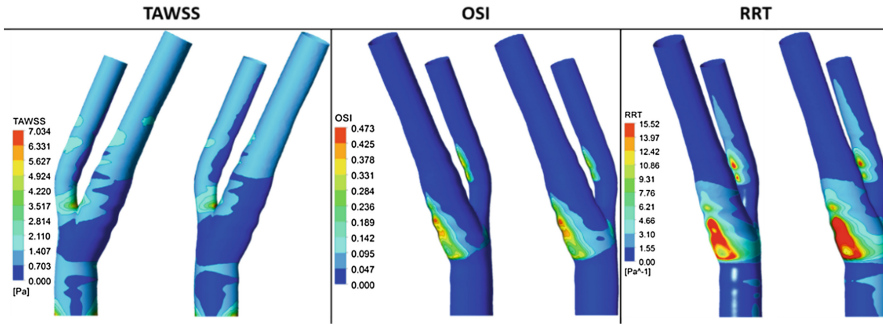
In this work two patients were studied, one, 57 years old, presenting a mild-graded stenosis along ICA with ECST grade of 50%, and another, 63 years old, with no visible stenosis. Figures 4, 5 and 6 show results corresponding to the non-stenosed carotid bifurcation. Velocity fields and streamlines obtained at systolic peak and mid deceleration cardiac cycle instants are presented in Fig. 4. This patient exhibited the highest velocities at ECA and stagnation zones are larger during mid-deceleration phase. Arterial walls deformation affects the flow behaviour, as in FSI model lower velocities, lower velocity gradients and greater recirculation zones were found in the bulb region of the ICA, opposite to the bifurcation divider wall, due to arterial wall elastic recovery.



**Fig. 4.** Non-stenosed carotid bifurcation: velocity fields and streamlines at systolic peak and mid deceleration cardiac cycle instants: rigid wall model (left) and flexible wall model (right).



**Fig. 5.** Non-stenosed carotid bifurcation: WSS contours at systolic peak instant: rigid wall model (left) and flexible wall model (right).



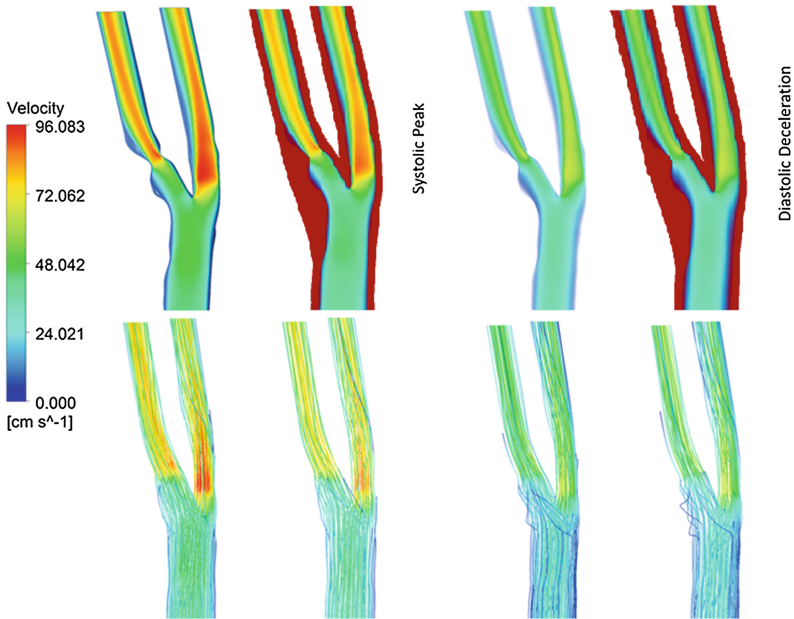
**Fig. 6.** Non-stenosed carotid bifurcation: WSS descriptors: rigid wall model (left) and flexible wall model (right).

Figure 5 shows WSS fields obtained at systolic peak instant. For the two models, the main features expected from fluid dynamics, such as low WSS values in the bulb region of the ICA, opposite to the bifurcation divider wall, corresponding to stagnation zone, and high WSS at the bifurcation apex, were successfully captured. The highest peak systolic WSS values were noticed in proximal ECA probably due to the vessel geometry. This study shows that compliance does little to affect WSS distribution.

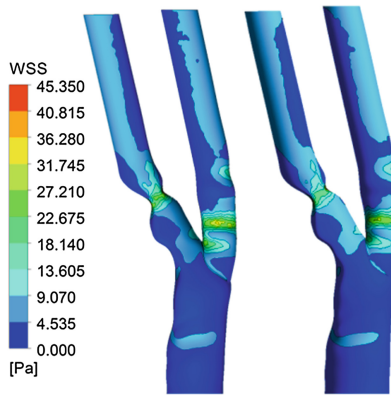
Figure 6 shows WSS descriptors, namely the time-averaged WSS (TAWSS) which evaluates the total shear stress exerted on the wall throughout a cardiac cycle, the oscillating shear index (OSI) that is used to identify regions on the vessel wall subjected to highly oscillating and the relative residence time of particles near the wall (RRT) a combination of the two previous ones. Both rigid and flexible models were able to capture flow disturbances at ICA origin, upstream and downstream stenosis and at ECA branch. FSI model shows lower TAWSS due to lower velocity gradient, and greater OSI and RRT values corresponding to greater turbulence. In Fig. 6 it can be seen that WSS hemodynamic factors distributions are similar for the two models and compliance does little to affect its distribution.

Figure 7 show velocity fields and streamlines obtained at systolic peak and mid deceleration cardiac cycle instants for the stenosed carotid bifurcation. As it was expected, the flow increases in vicinity of occlusion and recirculation can be noticed upstream and downstream stenosis. This recirculation zones are larger during mid-deceleration phase. Like in the previous example arterial walls deformation affects the flow behaviour.

WSS contours obtained at near peak systole instant are presented in Fig. 8. As expected low WSS values were found in the bulb region of the ICA, opposite to the bifurcation divider wall, corresponding to stagnation zone, and high WSS at the bifurcation apex, were successfully captured. Low WSS values were also found in the outer wall downstream stenosis identifying abnormal flow, due to the enlargement of the vessel. The highest peak systolic WSS values were noticed within the throat of ICA stenosis. A local increase in stress in the plaque region was captured by FSI model which could be a cause of atherosclerotic plaque rupture. This study shows that compliance affects WSS distribution.



**Fig. 7.** Stenosed carotid bifurcation: velocity fields and streamlines at systolic peak and mid deceleration cardiac cycle instants: rigid wall model (left) and flexible wall model (right)



**Fig. 8.** Stenosed carotid bifurcation: WSS contours at systolic peak instant: rigid wall model (left) and flexible wall model (right)

Figure 9 shows WSS descriptors. Both rigid and flexible models were able to capture flow disturbances at ICA origin, upstream and downstream stenosis and at ECA branch.



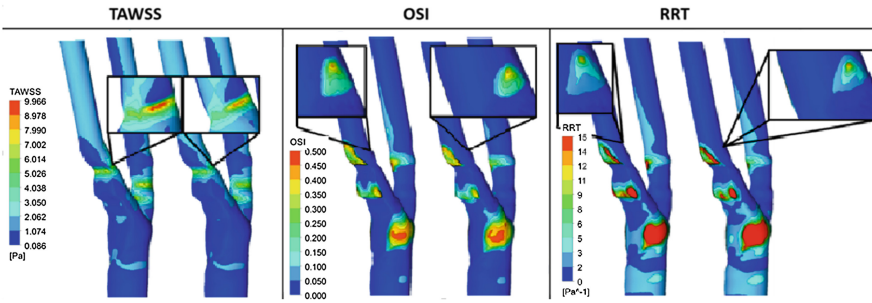


**Fig. 9.** Stenosed carotid bifurcation: WSS descriptors: rigid wall model (left) and flexible wall model (right).

FSI model shows lower TAWSS due to lower velocity gradient, and greater OSI and RRT values corresponding to greater turbulence. In Fig. 8 it can be seen that WSS hemodynamic factors distributions are similar for the two models and compliance does little to affect WSS descriptors distribution.

## 4 Conclusion

FSI analysis was performed based on in-vivo data, in order to investigate the influence of artery compliance on the CCA bifurcation hemodynamics and wall shear stress distribution. For the non-stenosed carotid bifurcation, WSS distribution is not affected by arterial wall compliance. Otherwise for the stenosed carotid bifurcation a local increase in stress in the plaque region was found; this could be a cause of plaque rupture and can be used for atherosclerotic plaque rupture risk assessment. In this study it is clear that deformation of vessel walls and atherosclerotic plaques are important factors affecting local hemodynamics in the proximal region of the CCA bifurcation. Further studies, should be performed in order to better understand the development and rupture of carotid atherosclerotic plaques.

**Acknowledgments.** The authors gratefully acknowledge the funding by FCT, Portugal, of the Research Unit of LAETA-INEGI, Faculdade de Engenharia da Universidade do Porto.

## References

1. Lee, S.W., Antiga, L., Steinman, D.A.: Correlations among indicators of disturbed flow at the normal carotid bifurcation. *J. Biomech. Eng.* **131**(6), 061013 (2009)
2. Sousa, L.C., Castro, C.F., António, C.C., Santos, A., Santos, R., Castro, P., Azevedo, E., Tavares, J.M.R.S.: Towards hemodynamic diagnosis of carotid artery stenosis based on ultrasound image data and computational modelling. *Med. Biolog. Eng. Comput.* **52**(11), 971–983 (2014)
3. Wootton, D., Ku, D.: Fluid mechanics of vascular systems, diseases, and thrombosis. *Annu. Rev. Biomed. Eng.* **1**, 299–329 (1999)



4. Gao, H., Long, Q., Graves, M., Gillard, J.H., Li, Z.I.: Carotid arterial plaque stress an analysis using fluid–structure interactive simulation based on in-vivo magnetic resonance images off our patients. *J. Biomech.* **42**, 1416–1423 (2009)
5. Huang, X., Yang, C., Yuan, C., Liu, F., Canton, G., Zheng, J., Woodard, P.K., Sicard, G.A., Tang, D.: Patient-specific artery shrinkage and 3D zero-stress state in multi-component 3D FSI models for carotid atherosclerotic plaques based on in vivo MRI data. *Mol. Cell. Biomech.* **6**(2), 121–134 (2009)
6. Leach, J.R., Rayz, V.L., Mofrad, M.R., Saloner, D.: An efficient two-stage approach for image-based FSI analysis of atherosclerotic arteries. *Biomech. Model. Mechanobiol.* **9**(2), 213–223 (2010)
7. Mulani, S.S., Jagad, P.I.: Analysis of the effects of plaque deposits on the blood flow through human artery. *Int. Eng. Res. J.* **2**, 253–260 (2015)
8. Tang, D., Yang, C., Zheng, J., Woodard, P.K., Saffitz, J.E., Sicard, G.A., Pilgram, T.K., Yuan, C.: Quantifying effects of plaque structure and material properties on stress distributions in human atherosclerotic plaques using 3D FSI models. *J. Biomech. Eng.* **127**(7), 1185–1194 (2005)
9. Zhao, S., Xu, X., Hughes, A., Thom, S., Stanton, A., Ariff, B., Long, Q.: Blood flow and vessel mechanics in a physiologically realistic model of a human carotid arterial bifurcation. *J. Biomech.* **33**, 975–984 (2000)
10. Dong, J., Sun, Z., Inthavong, K., Tu, J.: Fluid–structure interaction analysis of the left coronary artery with variable angulation. *Comput. Methods Biomech. Biomed. Eng.* **18**(14), 1500–1508 (2015)
11. Wong, K.K.L., Thavornpattanapong, P., Cheung, S.C.P., Sun, Z., Tu, J.: Effect of calcification on the mechanical stability of plaque based on a three-dimensional carotid bifurcation model. *Cardiovasc. Disord.* **12**(7), 1–18 (2012)
12. Henriques, H., Castro, C.F., Sousa, L.C., António, C.C., Santos, A., Santos, R., Castro, P., Azevedo, E.: Reconstructing stenotic carotid models from ultrasound images. In: Proceedings of the 6th International Conference on Mechanics and Materials in Design - M2D2015, pp. 1577–1580 (2015)
13. Sweet, W.L., Tio, F.O., Janicki, C., Duggan, D.M.: Measurement of density and calcium in human atherosclerotic plaque and implications for arterial brachytherapy. *Cardiovasc. Radiat. Med.* **1**(4), 358–367 (1999)